Stability of SiC and SiN interfaces in titanium carbide and nitride based heterostructures

Cite as: J. Appl. Phys. **125**, 075303 (2019); https://doi.org/10.1063/1.5082848
Submitted: 25 November 2018 . Accepted: 14 January 2019 . Published Online: 20 February 2019

V. I. Ivashchenko, P. E. A. Turchi, Leonid Gorb, Jerzy Leszczynski, N. R. Medukh, and R. V. Shevchenko

Journal of Applied Physics ARTICLE scitation.org/journal/jap

Stability of SiC and SiN interfaces in titanium carbide and nitride based heterostructures

Cite as: J. Appl. Phys. **125**, 075303 (2019); doi: 10.1063/1.5082848
Submitted: 25 November 2018 · Accepted: 14 January 2019 ·
Published Online: 19 February 2019

V. I. Ivashchenko,[1] P. E. A. Turchi,[2] Leonid Gorb,[3,4] Jerzy Leszczynski,[3] N. R. Medukh,[1] and R. V. Shevchenko[1,a)]

AFFILIATIONS

[1]Institute for Problems of Material Science NAS of Ukraine, Krzhyzhanovsky str. 3, 03142 Kyiv, Ukraine
[2]Lawrence Livermore National Laboratory, L-372, P.O. Box 808, Livermore, California 94551, USA
[3]Department of Chemistry and Biochemistry, Interdisciplinary Center for Nanotoxicity, Jackson State University, Jackson, Mississippi 39217, USA
[4]Badger Technical Services, LLC, Vicksburg, Mississippi 39180, USA

Note: This paper is part of the Special Topic on: Ultra-Hard Materials.
[a)]**Electronic mail:** shev@ipms.kiev.ua

ABSTRACT

First-principles molecular dynamics simulations of the stability of the NaCl-type (B1) SiC and SiN interfaces in TiX/one multilayer SiY (X,Y=C,N) heterostructures were carried out as functions of temperature. It was previously shown that the SiX interfaces in the heterostructures based on transition metal compounds could be dynamically unstable owing to the elongated interfacial Si-X bonds compared to the Si-X bonds in the B1-SiX phases in equilibrium. However, this criterion is not satisfied for some SiX(111) interfaces. The aim of this work is to study the temperature-induced changes in the structure of the heterostructures under consideration and to clarify a possible origin of instability of the interfaces in them. It is shown that, at finite temperatures, the interfacial layer in the TiN(001)/SiC heterostructure transforms into the zinc blende-type (B3) SiC-like layer, whereas the interfaces in other (001) heterostructures transform into amorphous-like interfacial layers. The TiC(111)/SiC and TiN(111)/SiN heterostructures are stable up to 1400 K. The TiN(111)/B3-like SiC and TiC(111)/B3-like SiN systems form during static relaxation of the initial heterostructures. The phase transformations of the interfaces are explained in terms of dynamical and elastic stability criteria. In contrast to the (111) interfacial layers, all the B1-(001) interfaces are found to be dynamically unstable. The formation of the B3-(111) interfaces occurs due to the elastic instability of the corresponding B1-(111) interface.

I. INTRODUCTION

Novel nanocomposites in the context of bulk materials and coatings were widely investigated in the past because of their unique mechanical properties.[1–3] Nanocomposite and nanolayered films based on transition metal nitrides and carbides demonstrate high hardness that is comparable to the hardness of diamond and high thermal stability, which makes them potential candidate materials for wear-resistant coating applications.[1,2,4,5] We are interested in such nanolayered systems and nanocomposites that contain titanium compounds and silicon compounds SiN_x and SiC. One of the plausible explanations of hardness enhancement in such nanocomposites is based on self-organized spinodal phase segregation, leading to nanocomposites that consist of crystallites of transition metal compounds with strong and one-layer interfaces of silicon compounds.[6,7] Thin SiC or SiN_x layers in superhard nanolayered coatings play an important role in strength enhancement.[8–11]

The SiN_x interface in the TiN-based nanocomposites was first assumed to be a very thin amorphous layer.[8] Then, this interface was considered as an epitaxial sub-stoichiometric B1−SiN_x layer stabilized between TiN(001) slabs.[9] In the nanolayered TiN/SiC films, the heteroepitaxial 3C–SiC layers were detected.[10,11] Nanocomposite coatings based on the TiC–SiC and TiC–SiN systems exhibit high hardness and wear-resistance.[12,13] These coatings represent the aggregation of

the TiC crystallites embedded into amorphous SiC or SiN_x matrices.

The stability of the interfaces in TiN(111)/Si_xN_y nanostructures was studied by using a first-principles approach.[14,15] The SiN, Si_2N_3, and Si_3N_4 structures were suggested as the plausible stable interfacial layers. The study of the dynamical and thermodynamic stability of a single monolayer of SiN_x between TiN(001) and TiN(111) slabs based on the density functional theory (DFT) showed that the (001) interface was dynamically instable, whereas the (111) interfacial layer was dynamically stable.[16] Both the interfaces were thermodynamically unstable with respect to Si vacancy formation.[16] Another interface SiN_x structure in TiN(001)/SiN_x was suggested in Ref. 17. It was shown that the 1-ML B3-drived SiN_x interface with a tetrahedral coordination between Si and N is stable with respect to both silicon and nitrogen vacancies. First-principles MD (FPMD) simulations were carried out to investigate the temperature effect on the stability of the SiN_x and SiC interfaces between the TiN slabs.[18,19] At finite temperature, the SiN(001) interface transforms into distorted octahedral SiN_6 and tetrahedral SiN_4 units aligned along the 110 directions. The B1-SiN, Si_3N_4-like SiN, and Si_3N_4-like Si_2N_3 interfaces between the TiN(111) slabs were stable up to 1400 K.[18] The FPMD calculations of the temperature stability of the TiN(001)/SiC and TiN(111)/SiC heterostructures showed that the B1-SiC(001) interface transformed into 3C-SiC-like layer at 700 K, in agreement with experiments,[10,11] and the formation of the 3C-SiC interfacial structure occurred during the static relaxation of the TiN(111)/B1-SiC heterostructure.[19] The SiC interface in the NbC(001)/SiC heterostructure was found to be an amorphous layer at high temperature, whereas the NbC(111)/SiC interface was stable up to 1400 K.[20] The DFT study of the mechanical properties of different TiN/SiN_x and TiN/SiC heterostructures was reported in Ref. 21. A simple approach for the estimation of the dynamical stability of the B1-SiN and B1-SiC interfaces in the heterostructures based on transition metal compounds was suggested in Ref. 22. It is based on the fact that an increase in the lattice parameter in B1-SiC and B1-SiN leads to an appearance of soft phonon modes.

Despite this, a fair amount of work models for describing the interface structures in TiC/SiC and TiC/SiN nanostructures are lacking, although they would provide highly needed information to design advanced nanocomposites and multilayer heterostructures with very promising wear-resistant coatings. Besides, the criterion[22] is not satisfied for the SiX(111) interfaces, since the Si-X bond lengths in both the (111) heterostructures and B1-SiX are comparable, and, despite this fact, some (111) interfaces undergo structural transformations.[19] To fill these gaps in studying the heterostructures based on TiC and TiN, we report on the results of first-principles results for TiX/SiY heterostructures (X, Y = C, N) that model corresponding nanocomposites. The TiC-based heterostructures are analyzed and compared with the TiN-based ones that were calculated earlier in Ref. 19. Heterostructure stability is investigated using dynamical and elastic stability criteria, and the simulation results are compared with available experimental models of the microstructures of nanocomposite and nanolayered films.

II. COMPUTATIONAL ASPECTS

To investigate the TiX(001)/SiY heterostructures (X, Y = C, N), we considered 96-atom supercells constructed of $(2 \times 2 \times 3)$–B1(NaCl)–TiN cubic unit cells each containing 8 atoms. The TiX(111)/1 ML SiY heterostructures consisted of 54-atom $(3 \times 3 \times 1)$ supercells, derived from the 6-atom B1–TiX hexagonal unit cells with $\left[\frac{1}{2}, \frac{1}{2}, 0\right]$, $\left[0, \frac{1}{2}, -\frac{1}{2}\right]$, and [1, 1, 1] as the *a*, *b*, and *c* basis vectors, respectively. The interfacial B1–SiX monolayer has been introduced by replacing Ti atoms with Si atoms in the central lattice planes of the given supercell. Thus, there are eight Si atoms and eight C atoms in the (001) interface, and nine Si atoms and nine C atoms in the (111) interface. (The latter heterostructure is "polar" in the *c*-direction). There are several parallel layers aligned perpendicularly to the *c*-direction, and one of them is the SiX interface in all the heterostructures.

The "QUANTUM ESPRESSO" code[23] with periodic boundary conditions was used to carry out first-principles calculations. The generalized gradient approximation (GGA) of Perdew, Burke, and Ernzerhof (PBE)[24] was selected for the exchange-correlation energy and potential, and Vanderbilt ultrasoft pseudopotentials were used to describe the electron-ion interaction.[25] The criterion of convergence for the total energy was $1.36 \cdot 10^{-5}$ eV/formula unit, and to speed up the convergence, each eigenvalue was convoluted by a Gaussian with a width of 0.272 eV. All the initial structures were optimized by simultaneously relaxing the atomic basis vectors and the atomic positions inside the unit cells using the Broyden-Fletcher-Goldfarb-Shanno (BFGS) algorithm.[26] The relaxation was considered to be complete provided the atomic forces were less than 25.7 meV/Å, the stresses smaller than 0.05 GPa, and the change in the total energy during the structural optimization was less than 1.36 meV. The cut-off energy for the plane-wave basis $E_{cut} = 408$ eV and the Monkhorst-Pack (2 2 2) mesh (4 *k*-points) were used.

Molecular dynamics (MD) simulations were performed as follows: the initial relaxed heterostructures were equilibrated at temperatures in the range of 300–1400 K during ~ 2.0 ps. For this, the constant number of particles-volume-temperature (NVT) ensemble was employed. The time step was 20 atomic units (about 10–15 s). The system temperature was kept constant in the range of ±50 K by rescaling velocities. During the initial 1–1.5 ps, all the structures reached closely their equilibrium state and, at later times, the total energy and cell volume varied only slightly around the constant equilibrium values. After the MD equilibration at 300 K, all the heterostructures were optimized using the BFGS algorithm.[26] The phonon dispersive curves and phonon density of states (PHDOS) were calculated in the framework of the density function perturbation theory (DFPT).[23] In these calculations, the *k*(electrons)- and *q*(phonon)-meshes were (6 6 4) and (3 3 2), respectively.

The stability of the heterostructures was analyzed in terms of dynamical and elastic stability criteria. A material is stable in the harmonic approximation without external load provided its phonon spectrum has real and positive frequencies (dynamical stability) and the elastic energy, given below, is always positive

$$E = E_0 + \frac{1}{2} V_0 \sum_{i,j=1}^{6} C_{ij} \varepsilon_i \varepsilon_j + O(\varepsilon^3),$$

where V_0 is the equilibrium volume of a crystal, ε denotes strain, and C_{ij} is a component of the matrix of second-order elastic constants. The latter condition is called the elastic stability criterion.[27] To investigate the phonon spectra and elastic stability of the (111) heterostructures, we generated the 6-atoms B1–TiX hexagonal unit cells with the SiY interfaces. These unit cells referred to as Ti2SiX2Y correspond to TiX(111)/B1-SiY heterostructures.

The calculated lattice parameter, a, for B1–TiC and B1–TiN (space group $Fm\bar{3}m$), B3-SiC (space group $F\bar{4}3m$), Si (space group $Fd\bar{3}m$), and C ($Fd\bar{3}m$) were 4.334 Å (4.330 Å, PDF [065–0971]), 4.247 Å (4.241 Å PDF [065–0565]), 4.378 Å (4.359 Å, PDF [029–1129]), 5.467 Å (5.431 Å, PDF [027–1402]), and 3.575 Å (3.567 Å, PDF [006–0675]), respectively (in parenthesis, the corresponding experimental lattice parameters are shown). The calculated values are slightly higher than the experimental ones because the GGA-PBE approximation tends to slightly overestimate structural parameters.[23]

III. RESULTS AND DISCUSSION

A. TiX(001)/SiY heterostructures

The heterostructures were investigated at various temperatures in the range of 0–1400 K. Figure 1 shows the dependence of the total energy (E_{tot}) on temperature of the TiX(001)/SiY heterostructures. Judging from the drastic reduction of E_{tot}, one can expect that all the heterostructures will undergo structural transformations. Below, it will be shown that the temperature-induced structural transformation occurs mainly in the interface region. The TiN(001)/SiC heterostructure turns out to be the most stable among other heterostructures: its total energy decreases significantly at high temperatures (higher than 700 K), whereas E_{etot} associated with other systems decreases abruptly already at very low temperatures. This result suggests that the TiN(001)/SiC heterostructure differs from other systems because of a unique mechanism of structural transformations. This result suggests that the TiN(001)/SiC heterostructure differs from other systems because of a unique mechanism of structural transformations that will be described below.

The atomic configurations of the TiC(001)/SiC and TiC(001)/SiN heterostructures generated at different temperatures are shown in Fig. 2. In Fig. 3, we show the atomic arrangement around the (001) interface in the high temperature TiC(001)/SiC and TiC(001)/SiN heterostructures. Because the (001) heterostructures are strongly influenced by

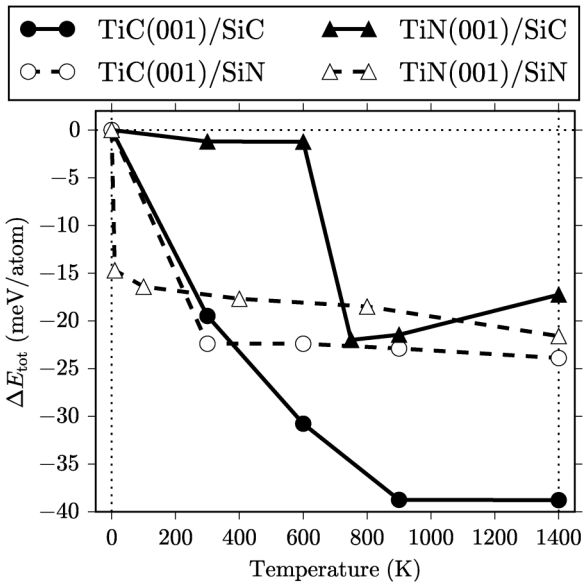

FIG. 1. Difference in total energies $\Delta E_{tot} = E_{tot}(T) - E_{tot}(0)$ for the TiX(001)/SiY heterostructures as a function of temperature, T.

temperature, we will focus on them. One can see that the initial relaxed TiC(001)/SiC heterostructure exhibits an epitaxial B1–SiC interfacial layer. An increase in temperature up 300 K leads to a significant change in the atomic arrangement caused by the thermal motion of the atoms within and near the interface. The redistribution of the atoms leads to the formation of the Si–C_3, Si–C_4, and Si–C_5 units. The C atoms form threefold coordinated graphite-like C–Si_3 configurations. A further increase in temperature leads to the formation of C–C_2Si configurations that are lacking in the low-temperature heterostructures (cf. Figs. 2 and 3). So, high

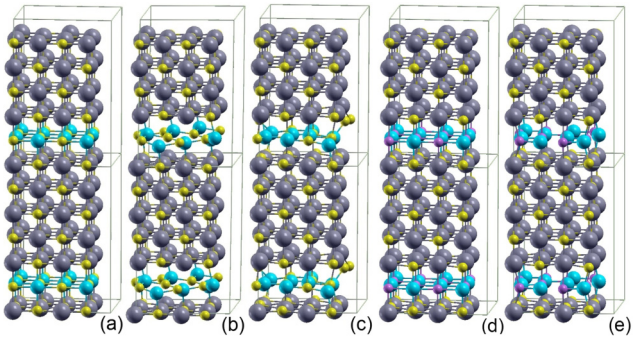

FIG. 2. Atomic configurations of the TiC(001)/SiC heterostructures generated at 0 K (a), 300 K (b), and 900 K (c), and the TiC(001)/SiN heterostructures generated at 0 K (d) and 900 K (e). The large grey, middle blue, small yellow, and small purple balls refer to Ti, Si, C, and N atoms, respectively.

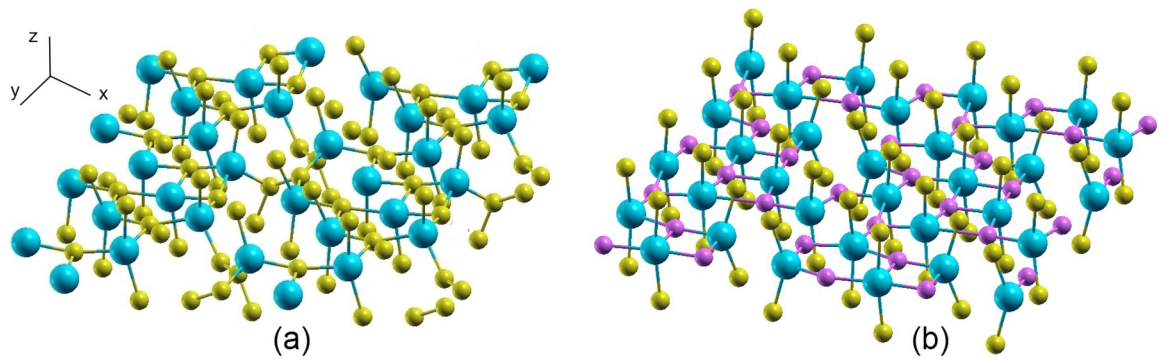

FIG. 3. Atomic configurations within and near the interface in the high temperature TiC(001)/SiC (a) and TiC(001)/SiN (b) heterostructures. Color associated with each atom type is the same as in Fig. 2.

temperatures promote the clustering of the interfacial carbon atoms. An analysis of the atomic configuration and total energy of the high temperature TiC(001)/SiC heterostructures during MD simulations shows that the formation of the carbon clusters is energetically favorable since results in a reduction in the total energy that is shown in Fig. 4 as a function of simulation time. The SiN(001) interfacial layer is more perfect compared to the SiC(001) interface (cf. Figs. 2 and 3) and consists of the distorted $Si-C_2N_2$ and $Si-C_2N_3$ units. Thus, both the interfaces can be considered as the amorphous-like interfacial layers.

For the sake of comparison, we note that a very similar interface structure was observed in TiN(001)/SiN heterostructures.[18] However, the B1-interface in the TiN(001)/SiC heterostructure transforms into the B3-like one at 700 K.[19] In Ref. 22, it was established that the SiC(001) interface is dynamically unstable in the heterostructures based on transition metal carbides and nitrides, provided the Si–C bond length (R_{Si-C}) in these heterostructures is larger than 2.135 Å. This rule is not satisfied for the TiN(001)/SiC heterostructure ($R_{Si-C} = 2.12$ Å), and therefore, this system is stable up to 700 K. A further increase in temperature leads to an increase of R_{Si-C} that causes a structural transformation of this interface. The SiN(001) interface will be dynamically unstable in all the heterostructures, since, for B1–SiN, the frequency of the Δ_5 mode [vibrations of atoms within the (001) plane] is imaginary within the wide range of lattice parameters.[22] The amorphous-like structure of the (001) interfaces is confirmed

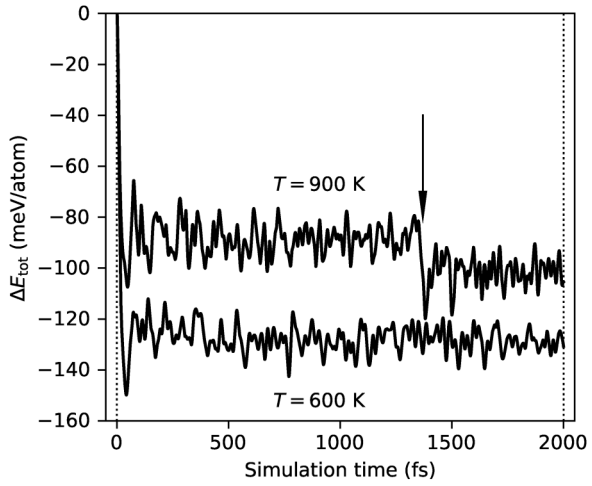

FIG. 4. Difference in total energies, $\Delta E_{tot} = E_{tot}(t) - E_{tot}(0)$, as a function of simulation time for the TiC(001)/SiC heterostructures generated at different temperatures. The arrow shows the one set of the carbon cluster formation in the heterostructure at 900 K.

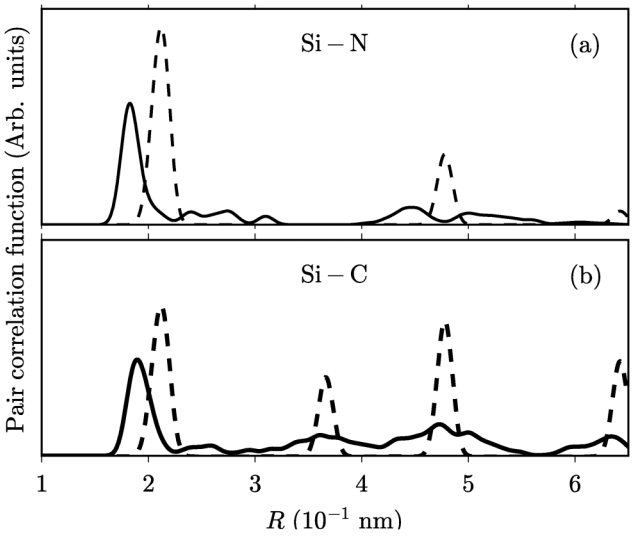

FIG. 5. Pair correlation functions for TiC(001)/SiN (a) and TiC(001)/SiC (b) heterostructures at $T = 0$ K (dashed line) and $T = 1400$ K (solid line).

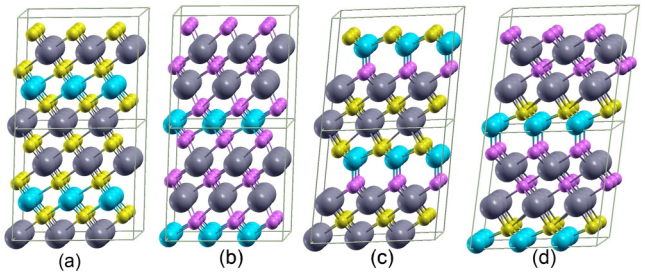

FIG. 6. Atomic configurations of the TiC(111)/SiC (a), TiN(111)/SiN (b), TiC(111)/SiN (c), and TiN(111)/SiC (d) heterostructures generated at 1400 K. Color associated with each atom type is the same as in Figs. 2 and 3.

by the results of the calculations of the pair correlation functions (PCF) presented in Fig. 5: only one peak of the nearest neighbor correlations is seen in the PCF for the high-temperature TiC(001)/SiC and TiC(001)/SiN heterostructures.

B. TiX(111)/SiY heterostructures

In Fig. 6, we show the atomic configurations of the high temperature TiX(111)/SiY heterostructures. The TiX(111) /SiX interfaces were found to be stable in the entire temperature range up to 1400 K. Due to the polar structure of the (111) heterostructure, the values of R_{Si-N} and R_{Si-C} in the relaxed TiC(111)/SiN and TiC(111)/SiC heterostructures decrease to 1.96 and 2.05 Å, respectively, to be compared with the bond length of 1.95 Å in TiN(111)/SiN and TiN (111)/SiC.[18,19] These values should be compared to the critical Si–N (1.95 Å) and Si–C (2.12 Å) bond lengths in B1–SiN and B1–SiC, respectively, for which a collapse of the Λ_3 phonon modes takes place.[22] We note that the bond lengths in the (111) heterostructures are comparable with the corresponding critical bond lengths. This means that the (111) heterostructures can be dynamically unstable. However, the presence of the Si–N–Ti and Si–C–Ti bonds in the (111) heterostructures could stabilize SiN(111) and SiC(111) interfaces. To verify this expectation, we calculate the phonon densities of states for the Ti2SiX2Y heterostructures, and the results are shown in Fig. 7. One can see that they do not contain imaginary frequencies. So, all the (111) heterostrucures are dynamically stable. However, the TiC(111)/SiN and TiN(111)/SiC interfaces undergo a B1–B3 structural transformation during static relaxation at 0 K. The latter is

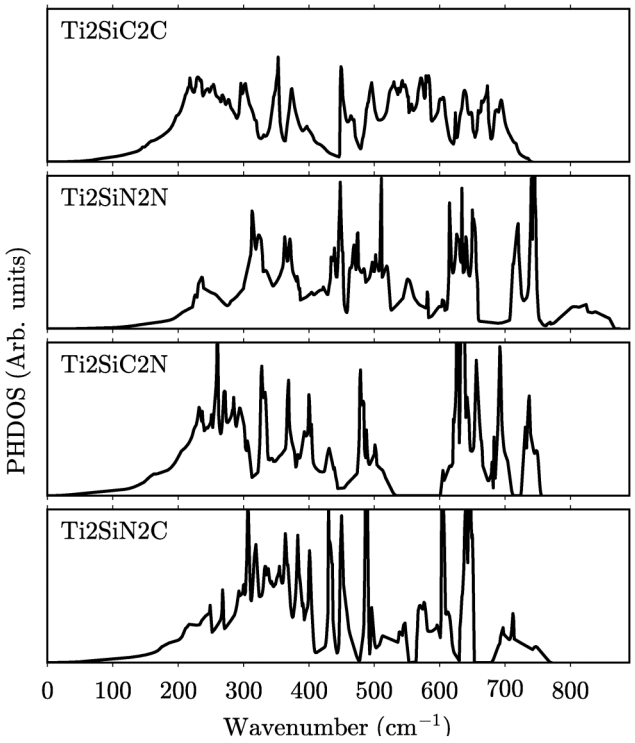

FIG. 7. Phonon density of states (PHDOS) for the TiX(111)/SiY 6-atom heterostructures (Ti2SiX2Y, X,Y=C,N). Denotation of the heterostructures was given in Sec. II.

unexpected, since all the TiX(111)/SiY heterostructures are dynamically stable. Then, the question arises—why are the Fig. 1. TiC(111)/SiN and TiN(111)/SiC interfaces unstable? To clarify this question, the elastic constants of the Ti2SiX2Y heterostructures were calculated. The results are presented in Table I. The following four necessary and sufficient conditions (criteria) for the elastic stability of a rhombohedral system (Point groups 32, $3m$, $\bar{3}m$)[27] are

$$\text{I.}\quad C_{11} > |C_{12}|,\ C_{44} > 0,$$

$$\text{II.}\quad C_{13}^2 < \frac{1}{2} C_{33}\,(C_{11} + C_{12}),$$

$$\text{III.}\quad C_{14}^2 < C_{44}\,C_{66}.$$

TABLE I. Elastic constants C_{ij} (in GPa) for the 6-atomic structures that model TiX(111)/SiY heterostructures (X, Y = C, N). Roman numerals I, II, and III denote the corresponding criteria presented in the text, with "Yes" if a criterion is satisfied and "No" if it is not. $C_{66} = \frac{1}{2}(C_{11} - C_{12})$.

Structure (symmetry)	C_{11}	C_{12}	C_{13}	C_{33}	C_{14}	C_{44}	C_{66}	I	II	III
Ti2SiC2C ($P\bar{3}m1$, 164)	495.2	144.7	129.1	471.3	34.0	91.9	175.3	Yes	Yes	Yes
Ti2SiN2N ($P\bar{3}m1$, 164)	505.6	157.5	137.0	498.1	6.1	175.8	174.0	Yes	Yes	Yes
Ti2SiC2N ($P3m1$, 156)	426.4	250.9	173.4	583.8	166.4	55.4	87.7	Yes	Yes	No
Ti2SiN2C ($P3m1$, 156)	435.8	223.3	120.0	559.8	122.5	74.8	106.2	Yes	Yes	No

One can see from Table I that, for the unstable (111) heterostructures, the criterion III is not satisfied. This fact explains why the dynamically stable TiC(111)/SiN and TiN(111)/SiC interfaces undergo a structural transformation. In terms of chemical bonding, the latter can be assigned to the asymmetrical C–Si–N neighborhood around the Si(111) layer.

We expect that this suggested explanation for the stability of the B1-interfaces in TiC and TiN-based heterostructures should be valid for other heterostructures with B1–SiC and B1–SiN interfacial layers. To confirm this hypothesis, the stability of the B1–SiC interfaces in the NbC/SiC heterostructures was recently explained using this approach.[20]

IV. CONCLUSIONS

The TiX(001)/SiY and TiX(111)/SY heterostructures (X, Y = C, N) were generated at different temperatures in the range of 0–1400 K using first-principles MD simulations with subsequent quenching to 0 K. The stability of the interfaces was considered by taking into account the dynamical stability of the B1–SiX phases at different lattice parameters. The B1–SiN phase is dynamically unstable in a wide range of lattice parameters, whereas the B1–SiC phase becomes unstable if the Si–C bond length exceeds 2.135 Å.[22] As a result, the SiN(001) interfaces and the TiC(001)/SiC interfacial layer are dynamically unstable and undergo a phase transformation from the B1 to amorphous-like structure. However, the interface in TiN(001)/SiC transforms to a B3-like layer. For this interface, R_{Si-C} is slightly lower than 2.135 Å, and the SiC(001) interface transforms into a B3-like layer only at high temperatures.

All the interfaces in TiX(111)/SiY turn out to be dynamically stable at all temperatures up to 1400 K. However, the interfaces in TiC(111)/SiN and TiN(111)/SiC transform into a B3-like layer during static relaxation, at 0 K. The stability of the (111) heterostructures is explained in terms of the elastic stability criterion. An analysis of the calculated elastic constants of the (111) heterostructures shows that, for the unstable (111) heterostructures, the elastic criterion stability is not satisfied.

In conclusion, these results should be useful to develop new high-performance nanocomposites and multilayered heterosystems based on transition metal compounds.

ACKNOWLEDGMENTS

This work was supported by the STCU (Contract No. #6372). The authors are grateful to the directorate of the Summer Institute at Jackson State University for the possibility to perform large-scale calculations.

REFERENCES

[1]S. Veprek, "Recent search for new superhard materials: Go nano!," Vac. Sci. Technol. A **31**, 050822 (2013).
[2]G. M. Demyashev, A. L. Taube, and E. Siores, "Superhard nanocomposites," in *Encyclopedia of Nanoscience and Nanotechnology*, edited by H. S. Nalwa (American Scientific Publishers, 2004), Vol. 10, pp. 191–236.
[3]J. Musil, "Hard and superhard nanocomposite coatings," Surf. Coat. Technol. **125**, 322–330 (2000).
[4]S. Veprek and M. J. G. Veprek-Heijman, "Industrial applications of superhard nanocomposite coatings," Surf. Coat. Technol. **202**, 5063–5073 (2008).
[5]S. Zhang, D. Sun, Y. Fu, and H. Du, "Recent advances of superhard nanocomposite coatings: A review," Surf. Coat. Technol. **167**, 113–119 (2003).
[6]S. Veprek, R. F. Zhang, M. G. J. Veprek-Heijman, S. H. Sheng, and A. S. Argon, "Superhard nanocomposites: Origin of hardness enhancement, properties and applications," Surf. Coat. Technol. **204**, 1898–1906 (2010).
[7]R. F. Zhang and S. Veprek, "On the spinodal nature of the phase segregation and formation of stable nanostructure in the ti–si–n system," Mater. Sci. Eng. A **424**, 128–137 (2006).
[8]S. Veprek and S. Reiprich, "Concept for the design of novel superhard coatings," Thin Solid Films **268**, 64–71 (1995).
[9]H. Söderberg, M. Odén, T. Larsson, L. Hultman, and J. M. Molina-Aldareguia, "Epitaxial stabilization of cubic-SiN_x in TiN/SiN_x multilayers," Appl. Phys. Lett. **88**, 191902-3 (2006).
[10]M. Kong, J. Dai, J. Lao, and G. Li, "Crystallization of amorphous sic and superhardness effect in tin/sic nanomultilayers," Appl. Surf. Sci. **253**, 4734–4739 (2007).
[11]A. D. Pogrebnjak, V. I. Ivashchenko, P. L. Skrynskyy, O. V. Bondar, P. Konarski, K. Zaleski, S. Jurga, and E. Coy, "Experimental and theoretical studies of the physicochemical and mechanical properties of multi-layered tin/sic films: Temperature effects on the nanocomposite structure," Compos. B Eng. **142**, 85–94 (2018).
[12]P. Eklund, J. Emmerlich, H. Högberg, O. Wilhelmsson, P. Isberg, J. Birch, P. O. A. Persson, U. Jansson, and L. Hultman, "Structural, electrical, and mechanical properties of *nc*–TiC/*a*-SiC nanocomposite thin films," J. Vac. Sci. Technol. B **23**, 2486–2495 (2005).
[13]S. Abraham, E. Y. Choi, N. Kang, and K. H. Kim, "Microstructure and mechanical properties of Ti–Si–C–N films synthesized by plasma-enhanced chemical vapor deposition," Surf. Coat. Technol. **202**, 915–919 (2007).
[14]S. Hao, B. Delley, and C. Stampfl, "Structure and properties of $TiN(111)/Si_xn_y/TiN(111)$ interfaces in superhard nanocomposites: First-principles investigations," Phys. Rev. B **74**, 035402-12 (2006).
[15]S. Hao, B. Delley, S. Veprek, and C. Stampfl, "Superhard nitride-based nanocomposites: Role of interfaces and effect of impurities," Phys. Rev. Lett. **97**, 086102-4 (2006).
[16]T. Marten, E. I. Isaev, B. Alling, L. Hultman, and I. A. Abrikosov, "Single-monolayer SiN_x embedded in TiN: A first-principles study," Phys. Rev. B **81**, 212102-4 (2010).
[17]T. Marten, B. Alling, E. I. Isaev, H. Lind, F. Tasnadi, L. Hultman, and I. A. Abrikosov, "First-principles study of the SiN_x/TiN(001) interfaces," Phys. Rev. B **85**, 104106-7 (2012).
[18]V. I. Ivashchenko, S. Veprek, P. E. A. Turchi, and V. I. Shevchenko, "Comparative first-principles study of TiN/SiN_x/TiN interfaces," Phys. Rev. B **85**, 195403-15 (2012).
[19]V. I. Ivashchenko, S. Veprek, P. E. A. Turchi, and V. I. Shevchenko, "First-principles study of TiN/SiC/TiN interfaces in superhard nanocomposites," Phys. Rev. B **86**, 014110-8 (2012).
[20]A. A. Onoprienko, V. I. Ivashchenko, I. I. Timofeeva, A. K. Sinelnitchenko, and O. A. Butenko, "Experimental and theoretical investigation of Nb–Si–C films," Surf. Coat. Technol. **300**, 35–41 (2016).
[21]S. Wang, R. Gudipati, A. S. Rao, T. J. Bostelmann, and Y. G. Shen, "First-principles calculations for the elastic properties of nanostructured superhard TiN/Si_xn_y superlattices," Appl. Phys. Lett. **91**, 081916-3 (2007).
[22]V. I. Ivashchenko and S. Veprek, "First-principles molecular dynamics study of the thermal stability of the Bn, AlN, SiC and SiN interfacial layers in TiN-based heterostructures: Comparison with experiments," Thin Solid Films **545**, 391–400 (2013).
[23]P. Giannozzi, S. Baroni, N. Bonini, M. Calandra, R. Car, C. Cavazzoni, D. Ceresoli, G. Chiarotti, M. Cococcioni, I. Dabo, A. D. Corso, S. de Gironcoli, S. Fabris, G. Fratesi, R. Gebauer, U. Gerstmann, C. Gougoussis, A. Kokalj, M. Lazzeri, L. Martin-Samos, N. Marzari, F. Mauri, R. Mazzarello, S. Paolini, A. Pasquarello, L. Paulatto, C. Sbraccia, S. Scandolo, G. Sclauzero,

A. Seitsonen, A. Smogunov, P. Umari, and R. Wentzcovitch, "Quantum espresso: A modular and open-source software project for quantum simulations of materials," J. Phys. Condens. Matter **21**, 395502 (2009).
[24]J. P. Perdew, K. Burke, and M. Ernzerhof, "Generalized gradient approximation made simple," Phys. Rev. Lett. **77**, 3865–3868 (1996).
[25]D. Vanderbilt, "Soft self-consistent pseudopotentials in a generalized eigenvalue formalism," Phys. Rev. B **41**, 7892–7895 (1990).
[26]S. R. Billeter, A. Curioni, and W. Andreoni, "Efficient linear scaling geometry optimization and transition-state search for direct wavefunction optimization schemes in density functional theory using a plane-wave basis," Comput. Mater. Sci. **27**, 437–445 (2003).
[27]F. Mouhat and F.-X. Coudert, "Necessary and sufficient elastic stability conditions in various crystal systems," Phys. Rev. B **90**, 224104-4 (2014).